FEMS Pathogens and Disease, 73, 2015, ftv009

doi: 10.1093/femspd/ftv009
Advance Access Publication Date: 6 February 2015
Research Article

RESEARCH ARTICLE

Chronic oral infection with major periodontal bacteria *Tannerella forsythia* modulates systemic atherosclerosis risk factors and inflammatory markers

Sasanka S. Chukkapalli[1], Mercedes F. Rivera-Kweh[1], Irina M. Velsko[1], Hao Chen[2], Donghang Zheng[2], Indraneel Bhattacharyya[3], Pandu R. Gangula[4], Alexandra R. Lucas[2] and Lakshmyya Kesavalu[1,5,*]

[1]Periodontology, College of Dentistry, University of Florida, Gainesville, FL 32610, USA, [2]Medicine and Molecular Genetics & Microbiology, College of Medicine, University of Florida, Gainesville, FL 32610, USA, [3]Oral Diagnostic Sciences, College of Dentistry, University of Florida, Gainesville, FL 32610, USA, [4]Department of Physiology, Department of Oral Biology and Research, School of Medicine and School of Dentistry, CWHR Nashville, TN 37208, USA and [5]Dept. of Periodontology and Oral Biology, College of Dentistry, University of Florida, Gainesville, FL 32610, USA

*Corresponding author: Department of Periodontology and Oral Biology, College of Dentistry, University of Florida, Gainesville, FL 32610-0424, USA. Tel: (352)-273-6500; Fax: (352)-273-6192; E-mail: Kesavalu@dental.ufl.edu

One sentence summary: Gum disease bacteria alter general risk factors including cholesterol levels.

Editor: Richard T. Marconi

ABSTRACT

Tannerella forsythia is a Gram-negative anaerobic organism that inhabits the subgingival cavity and initiates connective tissue destruction and alveolar bone resorption in periodontal disease (PD). PD is a chronic immunoinflammatory disease and has been linked to several systemic diseases including atherosclerosis. This study evaluated the effects of a chronic oral infection with *T. forsythia* ATCC 43037 on the induction of PD, inflammatory markers and atherosclerosis risk factors in hyperlipidemic ApoE^{null} mice. Mice were orally infected for 12 and 24 weeks prior to euthanasia. Bacterial colonization of the oral cavity and bacteremia was confirmed via isolation of genomic DNA from oral plaque and tissues. Oral infection elicited significantly elevated levels of serum IgG and IgM antibodies and alveolar bone resorption compared to control mice. *Tannerella forsythia*-infected mice had increased serum amyloid A, and significantly reduced serum nitric oxide when compared to controls. *Tannerella forsythia* chronic infection also significantly increased serum lipoproteins suggesting altered cholesterol metabolism and potential for aortic inflammation. Despite enhanced acute phase reactants and altered lipid profiles, *T. forsythia* infection was associated with decreased aortic plaque. This study investigates the potential of a known periodontal bacterial pathogen found in atherosclerotic plaque in humans to accelerate atherosclerosis in hyperlipdemic mice.

Keywords: *Tannerella forsythia*; atherosclerosis; ApoE^{null}; periodontal disease; atheromatous plaque

Received: 2 December 2014; **Accepted:** 22 January 2015

INTRODUCTION

Multispecies microbial communities form subgingival plaque in the oral cavity, and these communities establish within periodontal pockets and elicit inflammatory responses resulting in periodontal disease (PD Jenkinson and Lamont (2005)). PD is characterized by the destruction of the periodontal ligament, connective tissue and alveolar bone as a result of a chronic immune and inflammatory response following infection with a complex microbiome. It is unclear which pathogens initiate disease, but several species including *Porphyromonas gingivalis, Treponema denticola, Fusobacterium nucleatum, Aggregatibacter actinomycetemcomitans, Prevotella intermedia* and *Tannerella forsythia,* are associated in the destruction of the periodontium (Paster *et al.*, 2001). The consortium of bacteria most strongly implicated in the pathogenesis of PD is *P. gingivalis, T. denticola* and *T. forsythia,* all three of which are routinely found in subgingival plaque in patients with chronic periodontitis (Socransky *et al.*, 1998; Dashper *et al.*, 2011). Among these organisms, only *P. gingivalis* has been extensively investigated. Several studies indicate that PD pathogens are a contributing factor for numerous systemic diseases, including cardiovascular disease (CVD), diabetes, adverse pregnancy outcomes, rheumatoid arthritis and Alzheimer's disease (Mustapha *et al.*, 2007; Paquette, Brodala and Nichols 2007; Friedewald *et al.*, 2009; Kebschull, Demmer and Papapanou 2010; Zelkha, Frielich and Amar 2010). Recently, the American Heart Association reported that observational studies support an association between PD and atherosclerotic vascular disease but data do not as yet support a causal association (Lockhart *et al.*, 2012). Prior studies have indicated that factors linking coronary artery disease (CAD) and PD are independent of traditional CAD risk factors (Bahekar *et al.*, 2007; Humphrey *et al.*, 2008; Lockhart *et al.*, 2012), and hence it is imperative to investigate alternative risk factors to understand the more subtle and complex contributors to development of atherosclerosis.

During mastication, brushing, flossing and dental procedures periodontitis-associated bacteria from the oral cavity enter circulation. This transient and recurrent systemic bacterial insult may potentially contribute to vascular injury and inflammation that initiates atherogenesis (Forner *et al.*, 2006; Paquette, Brodala and Nichols 2007; Iwai 2009; Kebschull, Demmer and Papapanou 2010; Zelkha, Frielich and Amar 2010). In addition, multiple studies have also reported finding bacterial genomic 16S DNA belonging to known periodontal pathogens in atherosclerotic plaque (Haraszthy *et al.*, 2000; Kozarov *et al.*, 2006; Nonnenmacher *et al.*, 2007). Monoinfection with *P. gingivalis* has been implicated in acceleration of atherosclerotic lesions, and studies of a monoinfection with *P. gingivalis* or *T. denticola* in ApoE^{null} mice have documented genomic bacterial DNA in inflamed aortic tissue as well as modulation of inflammatory factors in association with bacterial infection and active invasion of the vessel wall (Li *et al.*, 2002; Lalla *et al.*, 2003; Gibson *et al.*, 2004; Hayashi *et al.*, 2010; Chukkapalli *et al.*, 2014; Velsko *et al.*, 2014). However, the impact of chronic oral infection with *T. forsythia* on atherogenesis is not yet known. Few studies have been performed looking at the pathogenicity of *T. forsythia* in animal models, specifically its atherogenic potential (Lee, Jun and Choi 2013; Rivera *et al.*, 2013).

Tannerella forsythia possess several virulence factors (Sharma 2010) including the surface antigen BspA (Sharma *et al.*, 1998), cell surface proteolytic enzymes (Grenier 1995; Saito *et al.*, 1997), a hemagglutinin (Murakami *et al.*, 2002), cell envelope lipoproteins (Hasebe *et al.*, 2004), glycosidases (Hughes *et al.*, 2003; Thompson *et al.*, 2009) and the cell surface (S)-layer (Sakakibara *et al.*, 2007) that contribute to its pathogenic potential. The S-layer has been shown to suppress T-helper 17 responses in dendritic cells and to increase alveolar bone resorption (ABR) in mice (Settem *et al.*, 2012b). The surface protein BspA can bind extracellular matrix components as well as other oral bacteria (Ikegami *et al.*, 2004; Sharma *et al.*, 2005), and is partially responsible for ABR (Sharma *et al.*, 2005). Recently, intravenous inoculation with *T. forsythia* or BspA was shown to enhance atherosclerosis progression in mice, perhaps by modulating lipid metabolism (Lee, Jun and Choi 2013).

Polymicrobial infections with *P. gingivalis, T. denticola, T. forsythia* and/or *F. nucleatum* as a mixed or monoinfection have been shown to synergistically enhance ABR in rats and mice (Kesavalu *et al.*, 2007; Verma *et al.*, 2010a,b; Settem *et al.*, 2012a) through physical, chemical and metabolic interactions as well as to accelerate atherosclerotic lesion development in mice (Sharma 2010; Rivera *et al.*, 2013). However, whether a chronic oral infection with *T. forsythia* alone can enhance PD, bacteremia, systemic inflammation and simultaneously accelerate atherosclerosis has not yet been examined. Additionally, a recent study reports a potential role for the microbiome, which would include oral bacteria, in immune responses and progression of disease (Honda and Littman 2012). Our study aimed to assess the effects of a monoinfection with *T. forsythia* on induction of PD as well as systemic infection leading to the invasion of vasculature and initiation of inflammatory atherosclerosis in an ApoE^{null} mouse model.

MATERIALS AND METHODS

Preparation of bacterial inoculum

Tannerella forsythia ATCC 43037 was cultured anaerobically at 37°C as described previously (Kesavalu *et al.*, 2007; Nahid *et al.*, 2011). The bacterial concentration was determined and cells were resuspended in reduced transport fluid (RTF) at 10^{10} cells per ml (Nahid *et al.*, 2011; Rivera *et al.*, 2013). *Tannerella forsythia* suspension in RTF was then mixed with equal volumes of 4% (w/v) sterile carboxy methylcellulose (CMC; Sigma-Aldrich, St. Louis, MO, USA) and this mixture was used for oral infection of ApoE^{null} mice as described previously (Chukkapalli *et al.*, 2014). Sham-infected mice were given a mixture containing equal parts of RTF and 4% CMC.

Oral infection and plaque sampling

Male ApoE^{null} mice (B6.129P2-ApoE$^{tm1Unc/J}$) were obtained from the Jackson Laboratory (Bar Harbor, ME, USA) and all mice procedures were performed in accordance with the approved protocol (201004539) guidelines set forth by the Institutional Animal Care and Use Committee of the University of Florida. The University of Florida has an Assurance with the Office of Laboratory Animal Welfare and follows Public Health Service policy, the Animal Welfare Act and Animal Welfare Regulations, and the National Institutes of Health Guide for the Care and Use of Laboratory Animals. The mice were anesthetized for 2–3 min using isoflurane inhalation anesthesia and 0.1 ml of *T. forsythia* suspension applied into the oral cavity as described (Rivera *et al.*, 2013). Oral infections were performed for 4 days (Monday–Thursday) once every 3 weeks (Fig. 1A). Oral plaque samples were taken 3 days following each infection using 0.1-inch-thick sterile cotton swabs. The swabs were suspended in 1:10 Tris-EDTA buffer for DNA isolation.

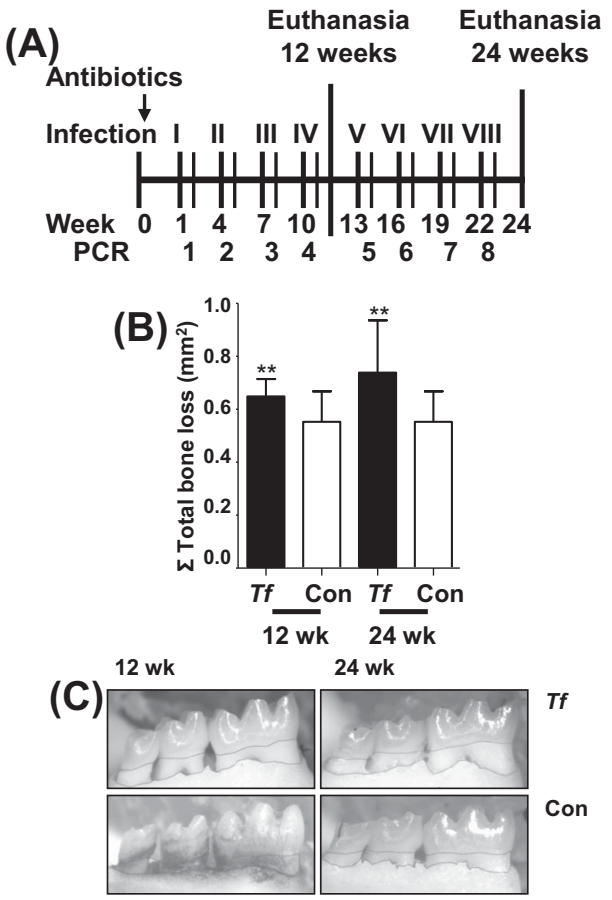

Figure 1. Chronic oral infection of ApoE^{null} mice with *T. forsythia* induces PD. (**A**) Schematic diagram of the experimental design illustrating eight total oral infections with *T. forsythia*, plaque sampling, PCR analysis and euthanasia (12 and 24 weeks). (**B**) Area of horizontal ABR in all jaw surfaces maxilla (buccal and palatal) and mandible (buccal). Each bar indicates the mean ABR ± SD for three molars in each quadrant of *T. forsythia* infected ($n = 12$) and control mice ($n = 12$). (**C**) Representative mandible lingual view of 12 and 24 weeks-infected and control mice with the area of bone resorption outlined from the CEJ to the ABC. *Tf - Tannerella forsythia*; con - control. $^{**}P < 0.005$ when compared to sham-infected controls.

Detection of *T. forsythia* genomic DNA in oral plaque

DNA was isolated from mouse oral plaque samples using the Wizard Genomic DNA Purification Kit (Promega, Madison, WI, USA) as described previously (Kesavalu *et al.*, 2007). PCR was performed as described (Rivera *et al.*, 2013) using 16S rRNA gene species-specific PCR oligonucleotide primers for *T. forsythia* (5′-AAAACAGGGGTTCCGCATGG-3′ (forward), 5′-TTCACCGCGGACTTAACAGC-3′ (reverse) (Kesavalu *et al.*, 2007).

Detection of *T. forsythia* genomic DNA in internal organs

DNA was isolated from infected and control mouse heart, liver, spleen, abdominal and thoracic aorta tissue samples using the DNeasy Blood and Tissue Kit (Qiagen, Valencia, CA, USA) and PCR was performed to detect *T. forsythia* genomic DNA as described above for oral plaque samples (Chukkapalli *et al.*, 2014).

Detection of *T. forsythia*-specific antibodies in mice serum

Serum from blood collected at euthanasia at 12 weeks and 24 weeks was used to determine immunoglobulin G (IgG) and IgM antibody concentrations against whole cell *T. forsythia* according to a standard ELISA protocol (Chukkapalli *et al.*, 2014). Mean *T. forsythia*-specific antibody titer values of infected mice were divided by mean antibody titer values of control mice, and the quotient represents the mean fold change in *T. forsythia*-specific antibody titer due to infection (Chukkapalli *et al.*, 2014). Graphs show mean fold change in *T. forsythia*-specific antibody titer of infected mice. Statistically significant differences between mean *T. forsythia*-specific antibody titers of infected and control groups were determined by two-tailed Student's *t* test, and are indicated above fold-change values on the graph.

Morphometric analysis of ABR

The horizontal ABR and the presence of intrabony defects were measured by morphometry (Bainbridge *et al.*, 2010; Rivera *et al.*, 2013). The area of horizontal ABR was measured using digital images of the buccal and lingual surfaces of all molars captured under a 10 × stereo dissecting microscope (SteReo Discovery V8; Carl Zeiss Micro imaging, Inc., Thornwood, NY, USA). The area of resorption was traced (using AxioVision LE 29A software version 4.6.3.) from the Cemento-enamel junction (CEJ) to the alveolar bone crest (ABC). Periodontal intrabony defects were also detected under a 10 × stereo dissecting microscope. The presence or absence of intrabony defects was detected in maxillae and mandibles stabilized with dental wax (Rivera *et al.*, 2013).

Morphometric analysis of aortic atherosclerosis

The heart, aortic arch, thoracic and abdominal aorta were harvested from infected and control mice. Specimens were then fixed in 10% neutral buffered formalin, processed and paraffin embedded as previously described (Lucas *et al.*, 1996; Bartee *et al.*, 2009; Dai *et al.*, 2010; Kesavalu *et al.*, 2012; Rivera *et al.*, 2013). Paraffin-embedded samples were cut transversely into 5 μm cross-sections (Leica microtome, RM2165 Microsystems Inc., Bannockburn, IL, USA). Hematoxylin-eosin-stained (H & E) sections were used for morphometric analysis. Plaque area as well as intimal and medial thickness were measured using an Olympus BX51 microscope (Olympus America, Center Valley, PA, USA) and the intimal to medial thickness ratios calculated as previously described (Velsko *et al.*, 2014).

Immunohistochemical analysis of inflammatory cell infiltration

Immunohistochemistry was performed to detect infiltration of the aortic tissue ($n = 6$ infected and control) with CD3$^+$ T cells and F4/80$^+$ macrophages as previously described (Velsko *et al.*, 2014). Positive cells were quantified in a 100 μm^2 area by a reviewer blinded to the groups.

Flow cytometric analysis of T cell subtypes

At 24-week sacrifice, whole spleens of six infected and six control mice were collected in RPMI-1640 supplemented with 10% FBS, 1% sodium pyruvate, 1% non-essential amino acids and 1%

L-glutamine (RPMI-complete). Spleens were homogenized and cells frozen in RPMI-complete-10% DMSO at –80°C for analysis. For flow cytometric analysis of T cell subtypes, frozen samples were thawed in a 37°C water bath, cell counts normalized to 10^5 Per 100 microliters in FACS buffer (PBS-1% FBS-0.1% EDTA) in wells of a FACS plate (Thermo Scientific, Waltham, MA, USA). The antibodies were added to wells at 1:100 and incubated for 30 min at 4°C. The antibodies detected the following targets: CD3-BrilliantViolet 421 (Biolegend 100227) to mark $CD3^+$ T cells, CD4-PE-Cy7 (eBioscience 25–0041) to mark $CD4^+$ T cells, IFNγRα-PE (eBioscience 12–1191) to mark Th1 cells, IL-4Rα-Fluorescein (R&D Systems FAB503F) to mark Th2 cells, and IL-17Rα-APC (eBioscience 17–7182) to mark Th17 cells. After incubation, cells were washed in FACS buffer, and fixed in 2% paraformaldehyde. Samples were detected on an LSR II flow cytometer (BD Biosciences) using FACSDiva software (BD Biosciences), and analysis performed using FCSExpress 4.0 software (DeNovo).

Serum nitric oxide (NO) and inflammatory biomarker serum amyloid A (SAA)

Serum from 24-week-infected ($n = 6$) and sham-infected ($n = 6$) mice was used to detect NO levels using a fluorometric assay kit (Bio Vision Inc., Milpitas, CA, USA), as described previously (Chukkapalli *et al.*, 2014). Serum from 24-week-infected ($n = 6$) and sham-infected ($n = 6$) mice was used to detect acute phase reactant SAA concentrations using the Mouse SSA ELISA kit (Kamiya Biomedical Company, Seattle, WA, USA) as previously described (Chukkapalli *et al.*, 2014).

Serum-oxidized LDL and lipoprotein evaluation

Serum from 24-week-infected ($n = 6$) and sham-infected ($n = 6$) mice was used to detect levels of oxidized LDL using the OLAb ELISA kit, (TSZ Scientific, Waltham, MA, USA). Serum lipoprotein levels (chylomicrons, VLDL, LDL and HDL), total cholesterol and total triglycerides from 24-week-infected ($n = 6$) and sham-infected ($n = 6$) mice were analyzed as described previously (Skylight Biotech Inc Akita, Japan) (Chukkapalli *et al.*, 2014).

Mouse atherosclerosis gene expression array

qRT-PCR was performed using the RT^2 Profiler Mouse Atherosclerosis PCR Array (SABiosciences, Valencia, CA, USA). Aortas ($n = 3$) of 24-week-infected and sham-infected mice were examined for expression levels of 84 pre-selected atherosclerosis-related genes (Chukkapalli *et al.*, 2014). RNA was extracted from homogenized samples using the RNeasy kit (Qiagen, Germantown, MD, USA), and then converted to cDNA using the RT^2 First Strand Kit (Qiagen, Germantown, MD, USA). cDNA was then added to the qPCR master mix and the mixture aliquotted into the PCR array plate. Thermal cycling was performed as per kit instructions.

Inflammatory cytokine expression detection

Sera from infected and sham-infected mice were pooled and used to detect 40 different cytokines using the Ray Biotech Mouse Inflammatory Cytokine glass chip Array (Ray Biotech, Inc., Norcross, GA, USA) as previously described (Chukkapalli *et al.*, 2014).

Detection of *T. forsythia* in infected tissue by fluorescent *in situ* hybridization (FISH)

FISH was performed on formalin-fixed paraffin-embedded right mandible tissue sections using Alexafluor-568 (Invitrogen, Carlsbad, CA, USA) labeled 16S rRNA oligonucleotide probes specific for *T. forsythia* 5′-CGTATCTCATTTTATTCCCCTGTA-3′ (Sunde *et al.*, 2003; Rudney, Chen and Sedgewick 2005). The protocol was performed as previously described (Velsko *et al.*, 2014).

Statistical analysis

Data except aortic histology and immunohistochemistry are presented as means ± standard deviations (SD). Aortic histology and immunohistochemistry are presented as means ± standard error mean (SEM). Unpaired, two-tailed Student's *t*-test was used to compare two independent groups. For all statistical analysis, Prism for Windows, version 5.0 (GraphPad Software, San Diego, CA, USA) or Statview statistics package were used ($P < 0.05$ considered significant).

RESULTS

Tannerella forsythia oral infection, PD induction and systemic dissemination

The oral cavity of $ApoE^{null}$ mice was swabbed 3 days after each infection to confirm colonization/infection by *T. forsythia*. PCR using bacterium-specific primers revealed all mice ($n = 24$) positive for *T. forsythia* genomic DNA following the third and fourth infection periods (Table 1). However, *T. forsythia* infection did not induce significant gingival pathology at either 12 or 24 weeks of infection (data not shown), nor were bacteria detected in gingival tissues by FISH (data not shown). ABR, the hallmark characteristic of PD, was significantly greater in *T. forsythia*-infected mice at both 12 and 24 weeks compared with sham-infected mice (Fig. 1B and C), demonstrating that infection-induced PD did develop in *T. forsythia*-infected mice. In addition, 14% of the total surface of both the mandibles and maxillae of *T. forsythia*-infected mice contained intrabony defects compared to 9% of the teeth surfaces of sham-infected mice at 12 and 24 weeks (Table 2), indicating development of intrabony defects resulting from infection.

Oral infection with *T. forsythia* induced a significant increase in immunoglobulin G (IgG) and immunoglobulin M (IgM)

Table 1. Distribution of $ApoE^{null}$ mice oral microbial samples positive for *T. forsythia* by PCR

	$n = 24$						$n = 12$	
No of Infections	1[a]	2	3	4	5	6	7	8
T. forsythia	0	0	24	24	0	0	0	2
Control	0	0	0	0	0	0	N/D	N/D

[a]Indicate number of infections at which oral microbial samples were collected to determine oral colonization by PCR. Infections 1–4 had $n = 24$ mice and infections 5–8 had $n = 12$ mice. Oral plaque samplings collected following each infection with *T. forsythia*. Samples were analyzed using appropriate *T. forsythia* species-specific PCR primers with positive and negative controls. Oral microbial samples were collected from sham-infected control mice and examined for *T. forsythia* genomic DNA using bacteria specific primers. N/D–samples were not collected. By the third and fourth infection, 100% of mice tested were positive for *T. forsythia* genomic DNA.

Table 2. *Tannerella forsythia* infection-induced intrabony defects in ApoE^{null} mice

Bacterial infection	% Intrabony defects* 12 weeks	24 weeks
T. forsythia	14%	14%
Control	9%	9%

*Percentage of tooth surfaces with periodontal intrabony defects.

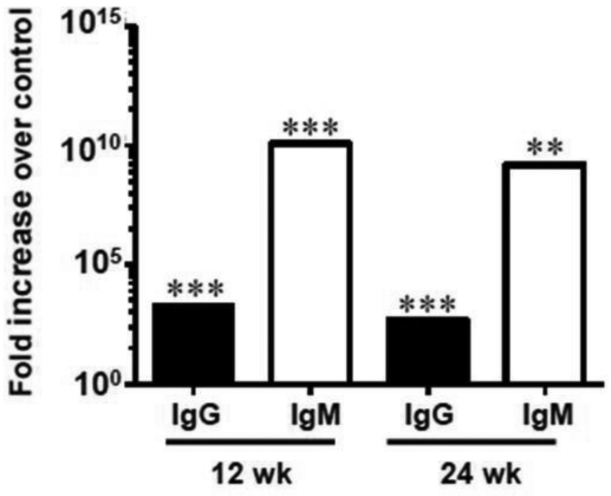

Figure 2. Oral infection induced a significant serum antibody response to *T. forsythia*. Serum IgG and IgM antibody levels from infected ApoE^{null} mice (collected at the end of 12 weeks and 24 weeks) showing fold increase in *T. forsythia*-specific antibody titers in infected mice over control mice at 12 and 24 weeks. $^{**}P < 0.005$, $^{***}P < 0.0001$.

antibody levels compared with that of sham-infected mice, a characteristic antibody response observed in periodontitis patients, further confirming that *T. forsythia*-induced specific immune response to infection. A significant 3-fold increase in IgG ($P < 0.0005$) and 10-fold increase IgM ($P < 0.0005$) levels resulted after 12 weeks of infection with *T. forsythia*. A significant 2-fold increase in IgG ($P < 0.0001$) and 8-fold increase in IgM ($P < 0.005$) levels resulted after 24 weeks of infection with *T. forsythia* (Fig. 2).

Additionally, the hematogenous dissemination of the bacteria into the heart, aorta, liver, spleen, kidney and lung was assessed by detecting the presence of *T. forsythia* genomic DNA by PCR using *T. forsythia*-specific primers. Infiltration of the heart (5 out of 12), aorta (2 out of 6), liver (6 out of 12) and lung (7 out of 12) was observed during 12 weeks of infection and aortic invasion was observed (6 out of 6) during 24 weeks of infection, confirming the invasion of *T. forsythia* in gingival epithelium and it's hematogenous dissemination to systemic organs (Table 3).

Histomorphometric analysis of atherosclerotic plaque after infection

Minimal atherosclerotic plaque was detected in the aortic arch, following 12 and 24 weeks of infection with *T. forsythia* (Fig. 3A–C), and a significant increase in plaque area ($P < 0.05$) was observed in sham-infected control mice at 24 weeks compared to infected mice (Fig. 3A). At 12 weeks, the intimal thickness of infected mice was slightly elevated, but by 24 weeks was significantly less than control mice (Fig. 3D, $P < 0.01$). In contrast, medial thickness was significantly higher in infected mice at 24 weeks compared to controls and to 12-week-infected mice (Fig. 3E, $P < 0.05$, $P < 0.01$). The intimal/medial thickness ratio of infected mice at 12 weeks was increased when compared to sham-infected mice, and decreased at 24 weeks of infection relative to sham-infected mice (Fig. 3F, $P < 0.01$).

Table 3. Detection of *T. forsythia* genomic DNA in ApoE^{null} mouse tissue

	12 weeks					
	Heart $n = 12$	Aorta $n = 6$	Liver $n = 12$	Spleen $n = 12$	Kidney $n = 12$	Lung $n = 12$
T. forsythia	5	2	6	0	0	7
Control	0	0	0	0	0	0
	24 weeks					
	Heart $n = 12$	Aorta $n = 6$	Liver $n = 12$	Spleen $n = 12$	Kidney $n = 12$	Lung $n = 12$
T. forsythia	0	6	0	0	0	0
Control	0	0	0	0	0	0

Hematogenous dissemination and invasion of *T. forsythia* in systemic organs were detected by presence of *T. forsythia* genomic DNA by PCR.

Twelve week-infected mice had significantly elevated CD3$^+$ T cells in the intimal layer of the aorta compared to controls (Fig. 4A $P < 0.001$), and by 24 weeks the CD3$^+$ T cell count were significantly increased in control mice compared to infected mice, and significantly less than 12-week-infected mice (Fig. 4A, $P < 0.001$). The adventitia of 12-week-infected mice had comparable numbers of CD3$^+$ T cells to controls, while by 24 weeks the CD3$^+$ T cells were again less than controls, but this was not significant (Fig. 4A and B). In control mice, the number of CD3$^+$ T cell count increased significantly at 24 weeks in both intimal and adventitial layers of aorta (Fig. 4C). Infiltrating F4/80$^+$ macrophage cells in the aorta were elevated in 12-week-infected mice in the intimal and medial arterial layers but this increase did not reach significance. In contrast, F4/80$^+$ macrophage cells were significantly elevated in the medial layer of the arterial wall compared to controls at 24 weeks ($P < 0.01$) (Fig. 4D). The infiltrating F4/80$^+$ macrophage cells were elevated in intimal layers of 24 week control mice (Fig. 4F) on comparison to infected mice (Fig. 4E). *Tannerella forsythia* was not detected by FISH in aortic vessel walls of infected mice either at 12 weeks or 24 weeks (data not shown).

Systemic inflammatory response to infection

Twenty four-week-infected mice did not demonstrate significantly elevated numbers of inflammatory CD3$^+$ CD4$^+$ IFNγ-receptor-positive splenic Th1 cells (Fig. 5A). In contrast, *T. forsythia*-infected mice exhibited significantly elevated numbers of CD3$^+$ CD4$^+$ IL-4-receptor-positive Th2 cells (Fig. 5B), which directly supports the enhanced humoral immune response induced by this pathogen. No differences in the number of inflammatory Th17 cells, characterized by the presence of IL-17 receptor (Fig. 5C), or the pathogenic IFNγ-receptor/IL-17-receptor-positive Th1/Th17 cells were detected in infected mouse spleens (Fig. 5D). These data further support that *T. forsythia* monoinfection does not promote strong systemic inflammation.

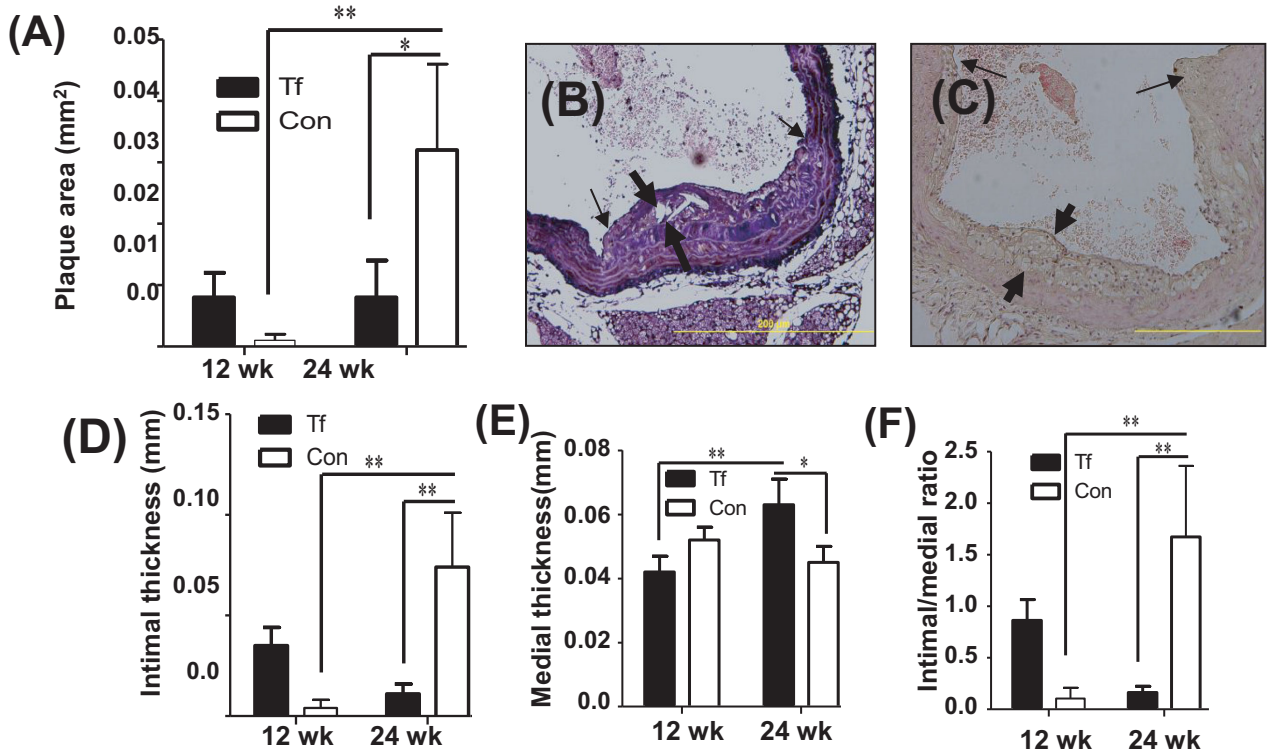

Figure 3. Chronic oral infection with *T. forsythia* does not promote atherosclerosis lesion formation. (**A**) Total aortic plaque area (mm^2) in 12 and 24 weeks *T. forsythia*-infected $ApoE^{null}$ mice compared to sham-infected mice. (**B**) Ascending aorta with small plaque in *T. forsythia*-infected mouse at 24 weeks with cholesterol crystals. (**C**) Ascending aortic cross-section at the level of aortic valve from 24-week sham-infected mouse. (**D**) Intimal thickness. (**E**) Medial thickness. (**F**) Intimal/medial thickness ratios. Thick arrows indicate plaque intimal thickness and thin arrows indicate plaque lateral margins. Six animals were examined in each group at both 12 and 24 weeks of infection. Multiple cross-sections were stained for measurement and analysis was performed three independent times by two separate individuals blinding to the treatment group. Bars show mean ± SEM. All graphs $n = 6$, $^{*}P < 0.05$, $^{**}P < 0.01$, $^{***}P < 0.001$.

Serum lipid profile alteration to infection

We determined the effects of *T. forsythia* oral infection for 24 weeks on induction of hyperlipidemia by analyzing serum lipoprotein content. The serum total cholesterol ($P < 0.05$) and triglyceride levels for *T. forsythia*-infected mice were significantly ($P < 0.05$) higher than sham-infected mice (Fig. 6A). *Tannerella forsythia* infection induced a significant ($P < 0.05$) increase in VLDL and LDL levels in comparison to sham-infected mice, as well as a significant ($P < 0.01$) increase in HDL levels (Fig. 6B), indicating that infection induced a hyperlipidemic state in $ApoE^{null}$ mice.

Infection-induced NO, SAA and oxidized LDL changes

To further determine the alteration in atherosclerosis risk factors induced by a chronic 24 week oral infection with *T. forsythia*, we analyzed serum NO levels and found a significant ($P < 0.001$) decrease in NO levels following infection, indicating endothelial dysfunction and a known precursor to atherosclerotic lesion development (Fig. 6C). Serum Amyloid A, an acute phase protein used as a biomarker of inflammatory burden and atherosclerosis risk showed a significant ($P < 0.01$) increase in infected mice when compared to the sham-infected mice (Fig. 6D), indicating elevated systemic inflammation. Levels of oxidized LDL were slightly but not significantly higher in *T. forsythia*-infected mice than control mice (Fig. 6E), suggesting an elevated potential for developing atherosclerotic lesions.

Atherosclerosis development-related gene expression changes

To investigate the effects of oral *T. forsythia* infection on atherosclerotic gene expression, we performed a PCR array examining expression of 84 genes known to be involved in atherogenesis. We observed a small number of those genes examined to have differing expression levels between infected mice and control mice (Table 4). The anti-apoptotic regulator gene *Birc3* exhibited a 30-fold increase, potentially indicating an attempt to control local apoptosis. Blood clotting/coagulation cascade molecules fibrinogen α chain (*Fga*) and fibrinogen β chain (*Fgb*) exhibited decreases in expression of 13-fold and 13-fold, respectively, while thrombosis-promoting *Serpinb2* showed a 5-fold increase in expression. We observed a decrease in *Il-1β* (-3.7-fold) that correlates with the minimal aortic plaque and inflammatory cell infiltration. We also observed a 5-fold decrease in *Ccl5*, a gene with a significant role in the inflammatory response, including chemotaxis of peripheral blood monocytes and activated T cells, further supporting an attempt at reduction of vascular inflammation. These changes do support potential for reduced plaque. Of the genes associated with lipid transport and metabolism that were examined, Apolipoprotein A1 (*ApoA1*) and *ApoB* expression were decreased relative to sham-infected mice

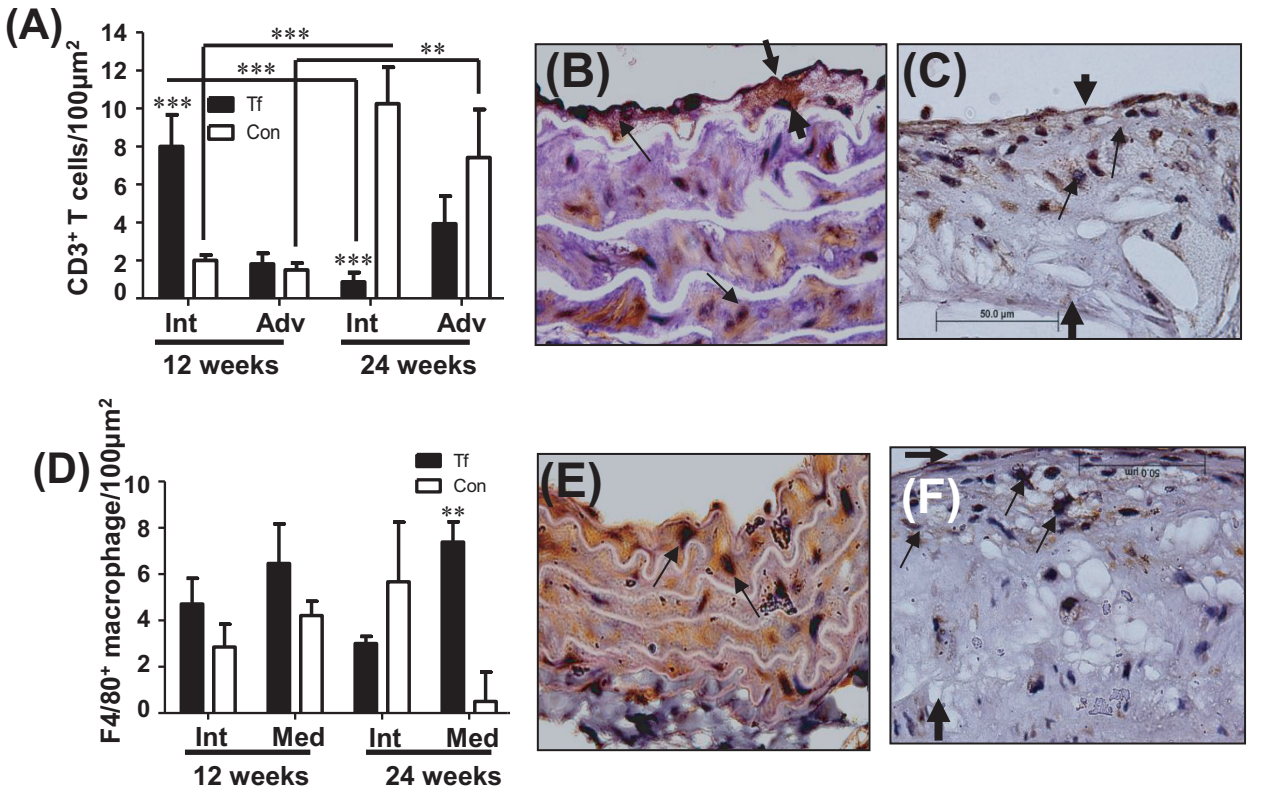

Figure 4. Immunohistochemical staining of aortic arterial cross-sections. **(A)** $CD3^+$ T cells in *T. forsythia*-infected and control mouse intimal and adventicial layers of aortas at 12 and 24 weeks of infection. **(B)** Immunohistochemical staining of aortic arterial cross-sections demonstrating few $CD3^+$ T cells in 24-week-infected mouse. **(C)** Sections demonstrating numerous $CD3^+$ T cells in 24-week sham-infected mouse. **(D)** $F4/80^+$ macrophage cell in *T. forsythia*-infected and control mouse intimal and medial layers of aortas at 12 and 24 weeks of infection. **(E)** Aortic arterial sections demonstrating few $F4/80^+$ macrophage cells in 24-week-infected mouse. **(F)** Aortic sections demonstrating numerous $F4/80^+$ macrophage cells in 24-week sham-infected mouse. A total of 6 mice were examined in each group at both 12 and 24 weeks of infection. Multiple cross-sections were stained for measurement and analysis was performed three independent times by two separate individuals blinding to the treatment. Small arrows point stained cells and thick arrows indicate plaque thickness. Bars show mean ± SEM. All graphs $n = 6$, $^*P < 0.05$, $^{**}P < 0.01$, $^{***}P < 0.001$.

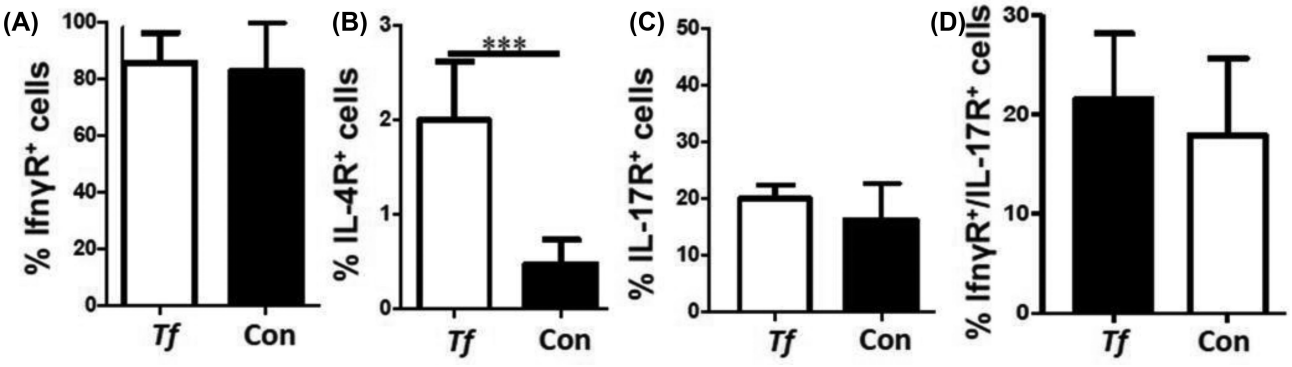

Figure 5. Flow cytometric analysis of 24 weeks *T. forsythia*-infected splenocytes. **(A)** No difference was found between infected and control mice IFNγ-receptor-positive $CD3^+$ Th1 T cells. **(B)** Infected mice have significantly elevated numbers of IL4-receptor-positive $CD3^+$ Th2 T cells. **(C)** No difference was found between infected and control mice $CD3^+$ Th17 T cells. **(D)** No difference was found between infected and control mice $CD3^+$ IFNγ-receptor/IL-17-receptor-positive Th1/Th17 T cells. $^{***}P < 0.001$.

by 10- and 5-fold, respectively, while transcription factors *Ppara* and *Rxra* were increased 2- and 2-fold, respectively (Table 4).

Changes in serum inflammatory mediators

To better understand the systemic inflammatory response to chronic oral *T. forsythia* infection, we examined the serum levels of 40 inflammatory cytokines. There were differences in the expression of inflammatory markers between 12- and 24-week-infected group (Table 5). Importantly, 12 weeks after infection mice exhibited a greater number of altered cytokines than 24-week-infected mice. The Th1 inflammation-promoting cytokines CD30L and IL12p40/p70 were upregulated 296- and 2790-fold, respectively, at 12 weeks but not significantly changed at 24 weeks of infection, supporting our gene expression data that suggest a reduction of inflammation is established. We observed

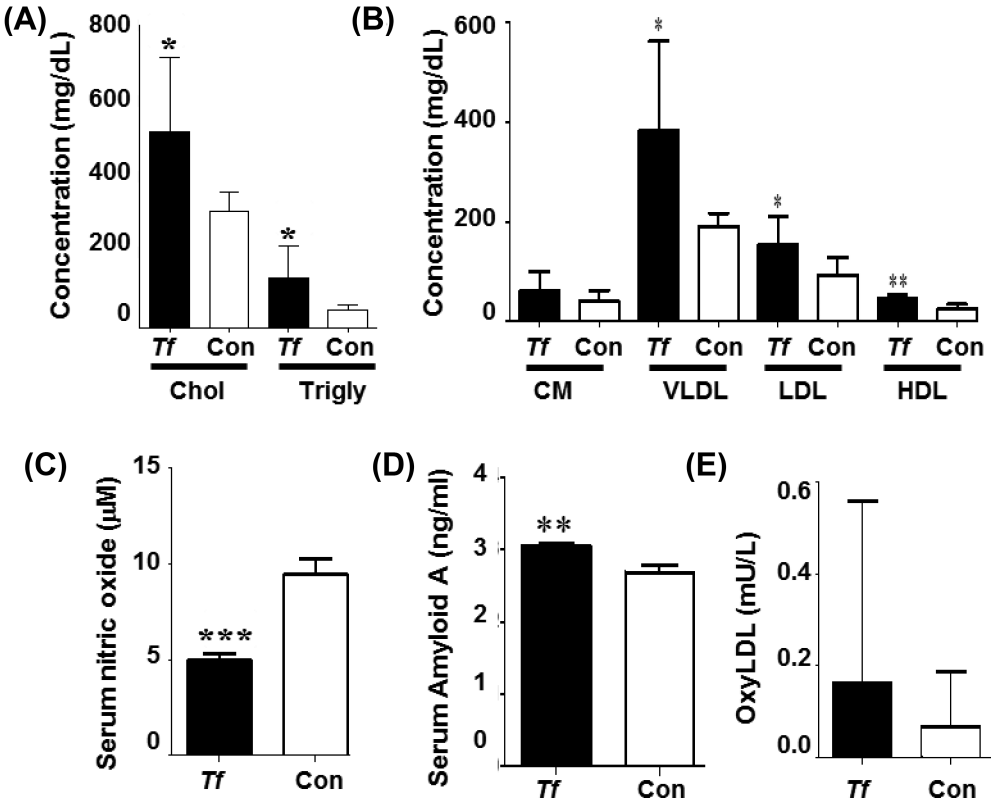

Figure 6. Serum risk factors for atherosclerosis are significantly altered by chronic *T. forsythia* infection. (**A**) Twenty-four weeks of infection significantly elevate total serum cholesterol and triglycerides. (**B**) Twenty-four weeks of infection significantly elevate very low-density lipoprotein (VLDL), low-density lipoprotein (LDL) and high-density lipoprotein (HDL) levels in *T. forsythia*-infected mice compared to sham-infected controls. (**C**) Serum nitric oxide is significantly decreased in infected mice compared to sham-infected controls at 24 weeks of infection. (**D**) SSA is significantly elevated in 24 weeks-infected mice compared to controls. (**E**) Serum-oxidized LDL (oxyLDL) levels are not significantly elevated in 24 weeks-infected mice relative to controls. *Tf* – *Tannerella forsythia*, Con – control. Bars show mean ± SD. All graphs $n = 6$, $^{*}P < 0.05$, $^{**}P < 0.01$, $^{***}P < 0.001$.

Table 4. *Tannerella forsythia* infection-induced altered expression of atherosclerosis genes

Gene grouping	Gene	Fold change
Apoptosis	*Bcl2a1a*	–2.17
	Birc 3	30.0
Blood clotting/coagulation cascade	*Fga*	–13.49
	Fgb	–13.18
	Npy	–6.57
	Serpinb2	4.52
	Serpine1	3.02
Immune response	*Ccl5*	–4.62
	Il-1α	2.25
	Il-1β	–3.70
	Il5	3.12
Leukocyte/endothelial cell adhesion	*Itga5*	2.22
	Sell	–3.09
Lipid transport and metabolism	*ApoA1*	–9.96
	ApoB	–5.43
	Ppara	2.13
	Rxra	2.28

Tannerella forsythia-infected and control aortic tissue samples at 24 weeks were processed and analyzed as described in the section 'materials and methods'.

a sustained Th2 response evidenced by elevated IL-4, up 191-fold at 12 weeks after infection and 50-fold at 24 weeks after infection. This is supported by the significant *T. forsythia*-specific antibody response observed at both 12 and 24 weeks of infection, and provides further evidence of a physiological attempt to reduce inflammation.

DISCUSSION

Recent *in vivo* studies have reported a causal link between *P. gingivalis*, and *T. denticola* monoinfections and atherogenesis in an $ApoE^{null}$ mouse model and have documented biological pathways in induction of inflammatory atherosclerosis (Gibson *et al.*, 2004; Miyamoto *et al.*, 2006; Chukkapalli *et al.*, 2014; Velsko *et al.*, 2014). However, human PD is always a chronic infection that is initiated by polymicrobial subgingival biofilm, which includes *P. gingivalis*, *T. denticola*, *T. forsythia*, *F. nucleatum* and *P. intermedia* (Socransky *et al.*, 1998; Pihlstrom, Michalowicz and Johnson 2005; Hajishengallis and Lamont 2012). Moreover, genomic DNA from nine periodontal bacteria has been detected in inflammatory atherosclerotic CVD lesions, further supporting a polymicrobial nature in atherosclerotic lesions (Haraszthy *et al.*, 2000), highlighting the importance of studying the role of oral pathogens other than *P. gingivalis* in induction of atherosclerosis. Although PD is complex and polymicrobial in nature, no single species has been implicated as primary etiological agent in PD, and the role and importance of each individual pathogen has yet to be examined. The aim of this study was to examine *in vivo* the capacity of one of the most frequently detected PD pathogens, *T. forsythia* (Dashper *et al.*, 2011), to cause gingival infection and induction

Table 5. *Tannerella forsythia* infection induced altered expression of serum inflammatory markers

	12 weeks		24 weeks	
Cytokine group	Cytokine	Fold difference	Cytokine	Fold difference
Cell activation and proliferation	**CD 30L**	**296**	IL1β	4.3
	INFγ	2.1	**IL4**	**49.9**
	IL1β	13.4	IL6	–2.0
	IL3	2.3	IL13	10.1
	IL4	191		
	IL9	2.1		
	IL10	2.4		
	IL12p40/p70	**2790**		
	IL17	2.3		
	IL-12p70	2.8		
	TNFα	2.1		
Leukocyte chemo attractants	TECK	2.0	Eotaxin	–2.8
	GSCF	8.1	KC	–4.9
	BLC	–2.5	LIX	–5.5
	MCP-1	5.0	SDF-1	–3.6
	Eotaxin	-3.3		
	LIX	–15.3		
T cell chemo attractants	Eotaxin-2	–5.4	Fas ligand	–3.2
	Fractalkine	2.4	Lymphotactin	2.8
	Fas ligand	3.3		
	MCSF	5.6		
	Lymphotactin	2.1		
	RANTES	2.0		
MMP inhibitor	TIMP-1	2.0		
	TIMP-2	3.2		
Others	Leptin	3.4		

Tannerella forsythia-infected mice sera ($n = 6$) and control mice sera ($n = 6$) at both 12 and 24 weeks was analyzed as described in the section 'materials and methods'. Bold entries indicate robust induction of cytokines. MMP—matrix metalloproteinase.

of periodontitis, as well as to assess the atherosclerotic potential of this pathogen.

Although *T. forsythia* was able to colonize the oral cavity of all the mice infected, colonization did not occur until the third infection and was not always sustained, unlike infection with the polymicrobial red complex (*P. gingivalis, T. denticola, T. forsythia*) which resulted in much earlier and more consistent colonization (Rivera *et al.*, 2013). There was also less gingival infiltration and inflammation seen on histological examination by *T. forsythia* alone (data not shown) when compared to infiltration and inflammation induced by the polymicrobial red complex pathogens (Rivera *et al.*, 2013), suggesting *in vivo* a dependent association of *T. forsythia* with *P. gingivalis* and *T. denticola* to induce pathogenicity. Chronic monoinfection with *T. forsythia* induced significant ABR and intrabony defects, indicating the establishment and progression of PD, providing direct evidence for its capacity to incite ABR, yet minimal junctional epithelial cell migration or inflammatory cell infiltration of connective tissue was observed. Therefore, we believe that although *T. forsythia* is capable of inducing PD symptoms in a mouse monoinfection model, a synergistic relationship between *T. forsythia* and other periodontal pathogens may be necessary to produce enhanced gingival pathology.

A majority of hearts, aortas, livers and lungs from 12-week-infected mice tested positive for genomic DNA of *T. forsythia*, indicating the potential to access systemic circulation and the aorta from the oral cavity. A recent review documented that *T. forsythia* possesses numerous virulence factors such as trypsin-like protease, PrtH protease, sialidases SiaH, NanH and a leucine-rich repeat cell-surface-associated protein BspA, which allow it to take advantage of the nutrients available in the periodontal pocket and to protect itself against immune attack (Sharma 2010). These virulence factors contribute to degradation of host gingival tissues, activate host degradative enzymes such as collagenase, modify host cell proteins for bacterial colonization, and cleave components involved in innate and adaptive immunity, thus paralyzing host immunity and activating components involved in ABR (Sharma 2010). We are unable to extrapolate whether these virulence factors are active in sites of systemic infection, as liver histology was normal when examined with H & E staining (data not shown).

Endothelial nitric oxide (NO) has been shown to have anti-atherogenic effects by preventing smooth muscle cell proliferation and leukocyte adhesion, and is considered an important molecule in the modulation of vascular disease (Matthys and Bult 1997; Channon, Qian and George 2000). Reduced NO production is a hallmark of a dysfunctional endothelium resulting from physical injury or oxidative stress; therefore, reduced levels of NO serve as an early marker of atherosclerosis (Meredith *et al.*, 1993). Although little aortic plaque was seen by histology, our study shows significantly reduced levels of NO in *T. forsythia*-infected mice, suggesting the possibility of vascular endothelial dysfunction. Reports suggest that infection with *T. forsythia* induces TNFα production, which affects NO production by reducing endothelial NO synthase expression (Yan *et al.*, 2008). *Tannerella forsythia*-induced TNFα is also known to alter reactive oxygen species, promoting oxidative stress (Kataoka *et al.*, 2010). However, we did not observe significantly elevated levels of oxidized LDL in sera of infected mice. The observed increase in levels of acute phase reactant SAA in infected mice shows a state

of acute inflammation being generated *in vivo*. Chronic inflammation and vascular endothelial dysfunction work in concert to promote atherogenesis. This study suggests *T. forsythia* infection decreases NO and increases the levels of serum acute phase reactant SAA, a biomarker of subclinical inflammation in chronic disorders such as atherosclerosis, rheumatic diseases, diabetes and obesity that are characterized by increased inflammation (Meek, Urieli-Shoval and Benditt 1994; Kumon *et al.*, 1999).

Although we observed an increase in total cholesterol and triglyceride levels at 24 weeks of infection, we also detected an increase in HDL levels, which is considered a 'good form of cholesterol'. HDL can be helpful in removing cholesterol and other lipid molecules, providing reverse lipid transport and therefore by nature is considered anti-atherogenic. This is also a possible explanation for the lack of atherosclerotic plaque formation in infected mice; however, further investigation is needed to determine how bacterial modulation of reverse lipid transport could reduce atherosclerotic plaque accumulation. Recently, it was shown that the BspA protein from *T. forsythia* is able to induce foam cell formation *in vivo* in THP-1 cells and accelerate the progression of atherosclerotic lesions *in vivo* in ApoE^{null} mice (Lee, Jun and Choi 2013), suggesting that *T. forsythia* is capable of inducing atherosclerotic plaque, specifically by interactions with its outer membrane protein BspA. However, the study utilized intravenous infection of *T. forsythia*, challenging the mice with a much higher bacterial level than our physiologically relevant oral infection model. As our model more accurately mimics the bacteremia levels experienced during PD and exposes mice to systemic levels of *T. forsythia* that are more physiologically relevant, it therefore supports our finding that oral *T. forsythia* infection alone is not sufficient to induce atherosclerosis.

Although pathogenesis of *T. forsythia* has not been as extensively studied as in other oral pathogens, certain bacterial components are known to strongly modulate immune responses. One example is the S-layer surface protein glycans which induce strong immune responses, modulate host immunity through Th17 suppression, enhance bacterial persistence and promote ABR (Sharma 2010; Settem *et al.*, 2012a,b). Modulation of the Th17-mediated pathway was evident in this study by a 2-fold decrease in IL-6 response at 24 weeks of infection. A Th1-mediated response in sera at 12 weeks of infection is evident by a 13-fold increase in IL-1β, a 2-fold increase in INFγ and a 2790-fold increase in IL-12, indicating that an inflammatory response is occurring, correlating with the observed increase in SAA, but is insufficient to drive aortic plaque development in this model. We observed a strong Th2-mediated response following 191-fold increase of IL-4 in 12 weeks infected mice, and 50-fold increase of IL-4 in 24 weeks infected mice, which corresponds with the significant serum humoral response and also a potential anti-inflammatory response.

There are reports about the significant role of the microbiome in modulating the immunological response of the host, especially various gut microflora (Hooper, Littman and Macpherson 2012; Kamada *et al.*, 2013). Due to the importance of the gut microbiota and dysbiosis in colitis disease pathogenesis, targeting the microbiota serves as an attractive therapeutic approach. In fact, faecal microbiota transplantation has been reported as highly effective in the treatment of *Clostridium difficile* infection (Borody and Khoruts 2011). This again suggests a similar significance of oral polymicrobial dysbiosis in development of atherosclerosis. However, it is as yet too early to speculate on the role of oral polymicrobial immune modulation and tolerance as sufficient observations are not available.

We have demonstrated increased oral ABR in response to *T. forsythia* infection together with increased serum markers of inflammation and altered serum lipid profile. Despite these increased risk factors for atherosclerosis progression, *T. forsythia* infection did not increase plaque growth in the aorta of ApoE^{null} mice. This study suggests that when grown as a monoculture, *T. forsythia* lacks the pathogenic capacity to drive atherosclerotic plaque development. As the natural niche for this species is a polymicrobial biofilm, growth in monoculture may induce expression of a set of genes distinct from those expressed in polymicrobial biofilm culture (Sarkar *et al.*, 2014; Tan *et al.*, 2014). It may be that as part of a biofilm community *T. forsythia* is more pathogenic and could contribute to atherosclerotic plaque development. Although it is difficult to establish the role of specific bacteria in a polymicrobial infection, studies support that synergism of the community rather than the specific effects of a single species drive disease pathogenesis (Hajishengallis *et al.*, 2011; Frias-Lopez and Duran-Pinedo 2012). Therefore, in humans the role of *T. forsythia*, or any individual oral bacterial species, in atherogenesis may be less important than its contribution to community pathogenesis.

FUNDING

This work was supported by NIH National Institute for Dental and Craniofacial Research (R01DE020820; Dr. Kesavalu); NIH National Center for Research Resources (1U54RR026140–01; Dr. Gangula).

Conflict of interest statement. None declared.

REFERENCES

Bahekar AA, Singh S, Saha S, *et al.* The prevalence and incidence of coronary heart disease is significantly increased in periodontitis: a meta-analysis. *Am Heart J* 2007;**154**:830–7.

Bainbridge B, Verma RK, Eastman C, *et al.* Role of *Porphyromonas gingivalis* phosphoserine phosphatase enzyme SerB in inflammation, immune response, and induction of alveolar Bone resorption in rats. *Infect Immun* 2010;**78**:4560–9.

Bartee MY, Dai E, Liu L, *et al.* 10 M-T7: measuring chemokine-modulating activity. *Method Enzymol* 2009;**460**:209–28.

Borody TJ, Khoruts A. Fecal microbiota transplantation and emerging applications. *Nat Rev Gastroentero* 2011;**9**:88–96.

Channon KM, Qian H, George SE. Nitric oxide synthase in atherosclerosis and vascular injury: insights from experimental gene therapy. *Arterioscl Thromb Vas* 2000;**20**:1873–81.

Chukkapalli SS, Rivera MF, Velsko IM, *et al.* Invasion of oral and aortic tissues by oral spirochete *Treponema denticola* in ApoE(−/−) mice causally links periodontal disease and atherosclerosis. *Infect Immun* 2014;**82**:1959–67.

Dai E, Liu LY, Wang H, *et al.* Inhibition of chemokine-glycosaminoglycan interactions in donor tissue reduces mouse allograft vasculopathy and transplant rejection. *PLoS One* 2010;**5**:e10510.

Dashper SG, Seers CA, Tan KH, *et al.* Virulence factors of the oral spirochete *Treponema denticola*. *J Dent Res* 2011;**90**:691–703.

Forner L, Larsen T, Kilian M, *et al.* Incidence of bacteremia after chewing, tooth brushing and scaling in individuals with periodontal inflammation. *J Clin Periodontol* 2006;**33**:401–7.

Frias-Lopez J, Duran-Pinedo A. Effect of periodontal pathogens on the metatranscriptome of a healthy multispecies biofilm model. *J Bacteriol* 2012;**194**:2082–95.

Friedewald VE, Kornman KS, Beck JD, *et al*. The American Journal of Cardiology and Journal of Periodontology Editors' Consensus: periodontitis and atherosclerotic cardiovascular disease. *Am J Cardiol* 2009;**104**:59–68.

Gibson FC, Hong C, Chou H-H, *et al*. Innate immune recognition of invasive bacteria accelerates atherosclerosis in apolipoprotein E-deficient mice. *Circulation* 2004;**109**:2801–6.

Grenier D. Characterization of the trypsin-like activity of *Bacteroides-Forsythus*. *Microbiology* 1995;**141**:921–6.

Hajishengallis G, Lamont RJ. Beyond the red complex and into more complexity: the polymicrobial synergy and dysbiosis (PSD) model of periodontal disease etiology. *Mol Oral Microbiol* 2012;**27**:409–19.

Hajishengallis G, Liang S, Payne MA, *et al*. Low-abundance biofilm species orchestrates inflammatory periodontal disease through the commensal microbiota and complement. *Cell Host Microbe* 2011;**10**:497–506.

Haraszthy VI, Zambon JJ, Trevisan M, *et al*. Identification of periodontal pathogens in atheromatous plaques. *J Periodontol* 2000;**71**:1–7.

Hasebe A, Yoshimura A, Into T, *et al*. Biological activities of *Bacteroides forsythus* lipoproteins and their possible pathological roles in periodontal disease. *Infect Immun* 2004;**72**:1318–25.

Hayashi C, Gudino CV, Gibson FC, III, *et al*. Pathogen-induced inflammation at sites distant from oral infection: bacterial persistance and induction of cell-specific innate immune inflammatory pathways. *Mol Oral Microbiol* 2010;**25**:305–16.

Honda K, Littman DR. The microbiome in infectious disease and inflammation. *Annu Rev Immunol* 2012;**30**:759–95.

Hooper LV, Littman DR, Macpherson AJ. Interactions between the microbiota and the immune system. *Science* 2012;**336**:1268–73.

Hughes CV, Malki G, Loo CY, *et al*. Cloning and expression of alpha-d-glucosidase and N-acetyl-beta-glucosaminidase from the periodontal pathogen, T*annerella forsythensis* (*Bacteroides forsythus*). *Oral Microbiol Immunol* 2003;**18**:309–12.

Humphrey LL, Fu R, Buckley DI, *et al*. Periodontal disease and coronary heart disease incidence: a systematic review and meta-analysis. *J Gen Intern Med* 2008;**23**:2079–86.

Ikegami A, Honma K, Sharma A, *et al*. Multiple functions of the leucine-rich repeat protein LrrA of *Treponema denticola*. *Infect Immun* 2004;**72**:4619–27.

Iwai T. Periodontal bacteremia and various vascular diseases. *J Periodontal Res* 2009;**44**:689–94.

Jenkinson HF, Lamont RJ. Oral microbial communities in sickness and in health. *Trends Microbiol* 2005;**13**:589–95.

Kamada N, Seo SU, Chen GY, *et al*. Role of the gut microbiota in immunity and inflammatory disease. *Nat Rev Immunol* 2013;**13**:321–35.

Kataoka H, Murakami R, Numaguchi Y, *et al*. Angiotensin II type 1 receptor blockers prevent tumor necrosis factor-alpha-mediated endothelial nitric oxide synthase reduction and superoxide production in human umbilical vein endothelial cells. *Eur J Pharmacol* 2010;**636**:36–41.

Kebschull M, Demmer RT, Papapanou PN. 'Gum bug, leave my heart alone!–' epidemiologic and mechanistic evidence linking periodontal infections and atherosclerosis. *J Dent Res* 2010;**89**:879–902.

Kesavalu L, Lucas AR, Verma RK, *et al*. Increased atherogenesis during *Streptococcus mutans* infection in ApoE-null mice. *J Dent Res* 2012;**91**:255–60.

Kesavalu L, Sathishkumar S, Bakthavatchalu V, *et al*. Rat model of polymicrobial infection, immunity, and alveolar bone resorption in periodontal disease. *Infect Immun* 2007;**75**:1704–12.

Kozarov E, Sweier D, Shelburne C, *et al*. Detection of bacterial DNA in atherornatous plaques by quantitative PCR. *Microbes Infect* 2006;**8**:687–93.

Kumon Y, Suehiro T, Hashimoto K, *et al*. Local expression of acute phase serum amyloid A mRNA in rheumatoid arthritis synovial tissue and cells. *J Rheumatol* 1999;**26**:785–90.

Lalla E, Lamster IB, Hofmann MA, *et al*. Oral infection with a periodontal pathogen accelerates early atherosclerosis in apolipoprotein E-null mice. *Arterioscler Thromb Vasc Biol* 2003;**23**:1405–11.

Lee H-R, Jun H-K, Choi B-K. *Tannerella forsythia* BspA increases the risk factors for atherosclerosis in ApoE(−/−) mice. *Oral Dis* 2013;**8**:803–8.

Li L, Messas E, Batista EL, *et al*. *Porphyromonas gingivalis* infection accelerates the progression of atherosclerosis in a heterozygous apolipoprotein E-deficient murine model. *Circulation* 2002;**105**:861–7.

Lockhart PB, Bolger AF, Papapanou PN, *et al*. Periodontal disease and atherosclerotic vascular disease: Does the evidence support an independent association?: A scientific statement from the American Heart Association. *Circulation* 2012;**125**:2520–44.

Lucas A, Liu L, Macen J, *et al*. Virus-encoded serine proteinase inhibitor SERP-1 inhibits atherosclerotic plaque development after balloon angioplasty. *Circulation* 1996;**94**:2890–900.

Matthys KE, Bult H. Nitric oxide function in atherosclerosis. *Mediat Inflamm* 1997;**6**:3–21.

Meek RL, Urieli-Shoval S, Benditt EP. Expression of apolipoprotein serum amyloid A mRNA in human atherosclerotic lesions and cultured vascular cells: implications for serum amyloid A function. *P Natl Acad Sci USA* 1994;**91**:3186–90.

Meredith IT, Anderson TJ, Uehata A, *et al*. Role of endothelium in ischemic coronary syndromes. *Am J Cardiol* 1993;**72**:27C–31C.

Miyamoto T, Yumoto H, Takahashi Y, *et al*. Pathogen-accelerated atherosclerosis occurs early after exposure and can be prevented via immunization. *Infect Immun* 2006;**74**:1376–80.

Murakami Y, Higuchi N, Nakamura H, *et al*. *Bacteroides forsythus* hemagglutinin is inhibited by N-acetylneuraminyllactose. *Oral Microbiol Immunol* 2002;**17**:125–8.

Mustapha IZ, Debrey S, Oladubu M, *et al*. Markers of systemic bacterial exposure in periodontal disease and cardiovascular disease risk: a systematic review and meta-analysis. *J Periodontol* 2007;**78**:2289–302.

Nahid MA, Rivera M, Lucas A, *et al*. Polymicrobial infection with periodontal pathogens specifically enhances microRNA miR-146a in ApoE−/− mice during experimental periodontal disease. *Infect Immun* 2011;**79**:1597–605.

Nonnenmacher C, Stelzel M, Susin C, *et al*. Periodontal microbiota in patients with coronary artery disease measured by real-time polymerase chain reaction: a case-control study. *J Periodontol* 2007;**78**:1724–30.

Paquette DW, Brodala N, Nichols TC. Cardiovascular disease, inflammation, and periodontal infection. *Periodontol 2000* 2007;**44**:113–26.

Paster BJ, Boches SK, Galvin JL, *et al*. Bacterial diversity in human subgingival plaque. *J Bacteriol* 2001;**183**:3770–83.

Pihlstrom BL, Michalowicz BS, Johnson NW. Periodontal diseases. *Lancet* 2005;**366**:1809–20.

Rivera MF, Lee JY, Aneja M, *et al*. Polymicrobial infection with major periodontal pathogens induced periodontal disease and aortic atherosclerosis in hyperlipidemic ApoE(null) mice. *PLoS One* 2013;**8**:e57178.

Rudney JD, Chen R, Sedgewick GJ. *Actinobacillus actinomycetemcomitans*, *Porphyromonas gingivalis*, and *Tannerella forsythensis* are components of a polymicrobial intracellular flora within human buccal cells. *J Dent Res* 2005;**84**:59–63.

Saito T, Ishihara K, Kato T, *et al*. Cloning, expression, and sequencing of a protease gene from *Bacteroides forsythus* ATCC 43037 in Escherichia coli. *Infect Immun* 1997;**65**:4888–91.

Sakakibara J, Nagano K, Murakami Y, *et al*. Loss of adherence ability to human gingival epithelial cells in S-layer protein-deficient mutants of *Tannerella forsythensis*. *Microbiology* 2007;**153**:866–76.

Sarkar J, McHardy IH, Simanian EJ, *et al*. Transcriptional responses of *Treponema denticola* to other oral bacterial species. *PLoS One* 2014;**9**:e88361.

Settem RP, El-Hassan AT, Honma K, *et al*. *Fusobacterium nucleatum* and *Tannerella forsythia* induce synergistic alveolar bone loss in a mouse periodontitis model. *Infect Immun* 2012a;**80**:2436–43.

Settem RP, Honma K, Nakajima T, *et al*. A bacterial glycan core linked to surface (S)-layer proteins modulates host immunity through Th17 suppression. *Mucosal Immunol* 2012b;**6**:415–26.

Sharma A. Virulence mechanisms of *Tannerella forsythia*. *Periodontol. 2000* 2010;**54**:106–16.

Sharma A, Inagaki S, Honma K, *et al*. *Tannerella forsythia*-induced alveolar bone loss in mice involves leucine-rich-repeat BspA protein. *J Dent Res* 2005;**84**:462–7.

Sharma A, Sojar HT, Glurich I, *et al*. Cloning, expression, and sequencing of a cell surface antigen containing a leucine-rich repeat motif from Bacteroides forsythus ATCC 43037. *Infect Immun* 1998;**66**:5703–10.

Socransky SS, Haffajee AD, Cugini MA, *et al*. Microbial complexes in subgingival plaque. *J Clin Periodontol* 1998;**25**:134–44.

Sunde PT, Olsen I, Göbel UB, *et al*. Fluorescence in situ hybridization (FISH) for direct visualization of bacteria in periapical lesions of asymptomatic root-filled teeth. *Microbiology* 2003;**149**:1095–102.

Tan KH, Seers CA, Dashper SG, *et al*. *Porphyromonas gingivalis* and *Treponema denticola* exhibit metabolic symbioses. *PLoS Pathog* 2014;**10**:e1003955.

Thompson H, Homer KA, Rao S, *et al*. An orthologue of *Bacteroides fragilis* NanH is the principal sialidase in *Tannerella forsythia*. *J Bacteriol* 2009;**191**:3623–8.

Velsko IM, Chukkapalli SS, Rivera MF, *et al*. Active invasion of oral and aortic tissues by *Porphyromonas gingivalis* in mice causally links periodontitis and atherosclerosis. *PLoS One* 2014;**9**:e97811.

Verma RK, Bhattacharyya I, Sevilla A, *et al*. Virulence of major periodontal pathogens and lack of humoral immune protection in a rat model of periodontal disease. *Oral Dis* 2010a;**16**:686–95.

Verma RK, Rajapakse S, Meka A, *et al*. *Porphyromonas gingivalis* and *Treponema denticola* mixed microbial infection in a rat model of periodontal disease. *Interdiscip Perspect Infect Dis* 2010b;**2010**:605125.

Yan G, You B, Chen S-P, *et al*. Tumor necrosis factor-alpha downregulates endothelial nitric oxide synthase mRNA stability via translation elongation factor 1-alpha 1. *Circ Res* 2008;**103**:591–7.

Zelkha SA, Frielich RW, Amar S. Periodontal innate immune mechanisms relevant to atherosclerosis and obesity. *Periodontol 2000* 2010;**54**:207–21.